Electronic Supplementary Material (ESI) for Nanoscale.

Supporting Information

Reconfigurable Label-Free Shape-Sieving of Submicron Particles in Chalcogenide Waveguide Array

Tun Cao*, Zhongming Wang, and Libang Mao

*Corresponding Author: caotun1806@dlut.edu.cn

School of Optoelectronic Engineering and Instrumentation Science, Dalian University of Technology, Dalian 116024, China

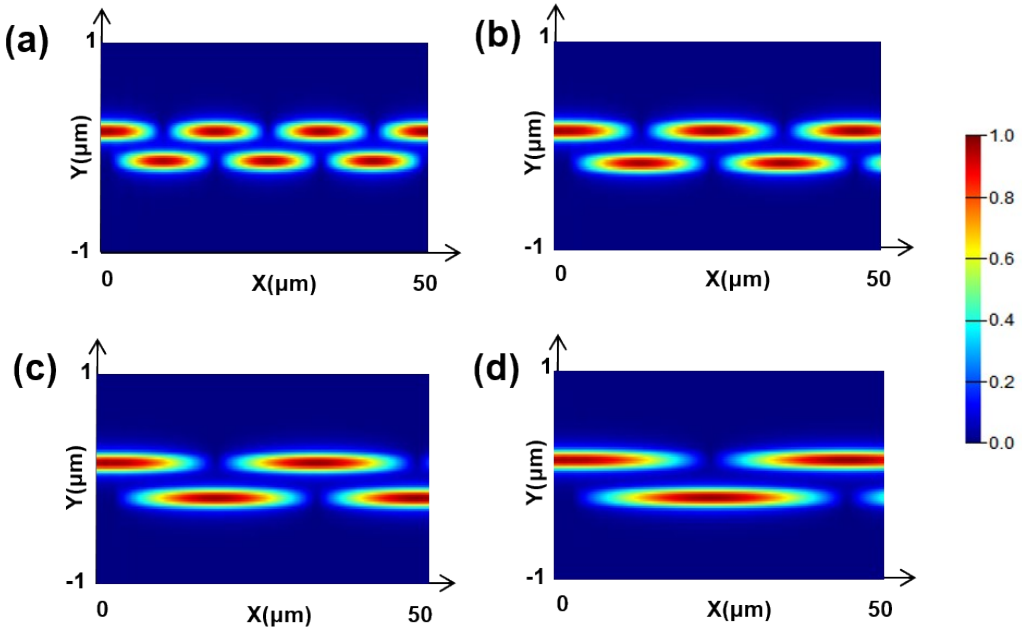

Fig. S1 A variety of electric (*E*-) field intensity distributions in the paired amorphous Sb_2Se_3 waveguides under the different distance of (a) G= 200 nm, (b) G= 250 nm, (c) G= 300 nm, and (d) G= 350 nm.

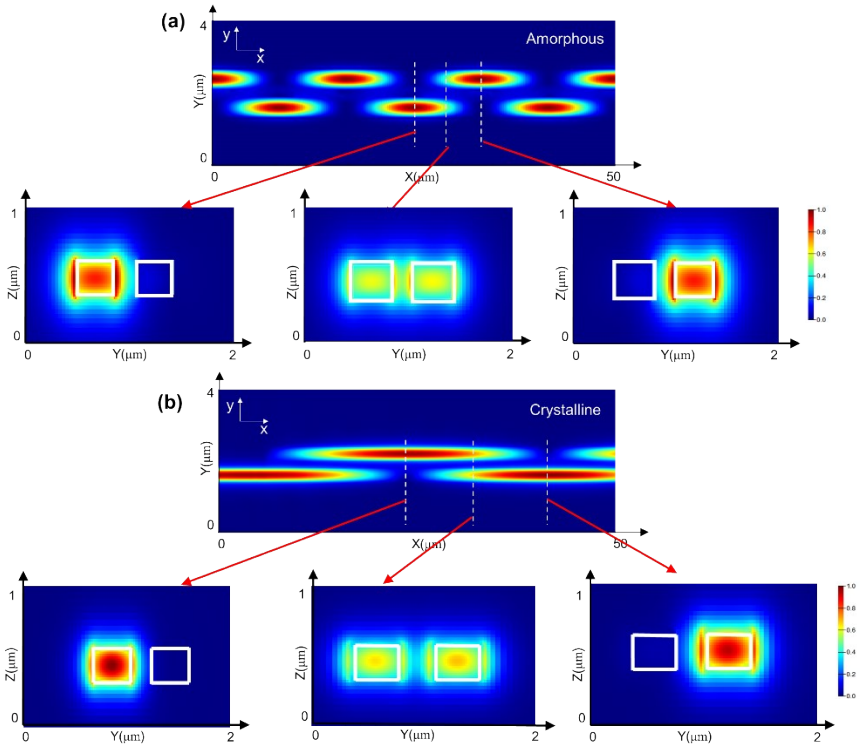

Fig. S2 The normalized *E*-field intensity distributions of the paired Sb_2Se_3 waveguides along the *y*-*z* plane at λ= 1.55μm for both (a) amorphous and (b) crystalline states, respectively. The left, central, and right columns present the normalised *E*-field intensity distributions.

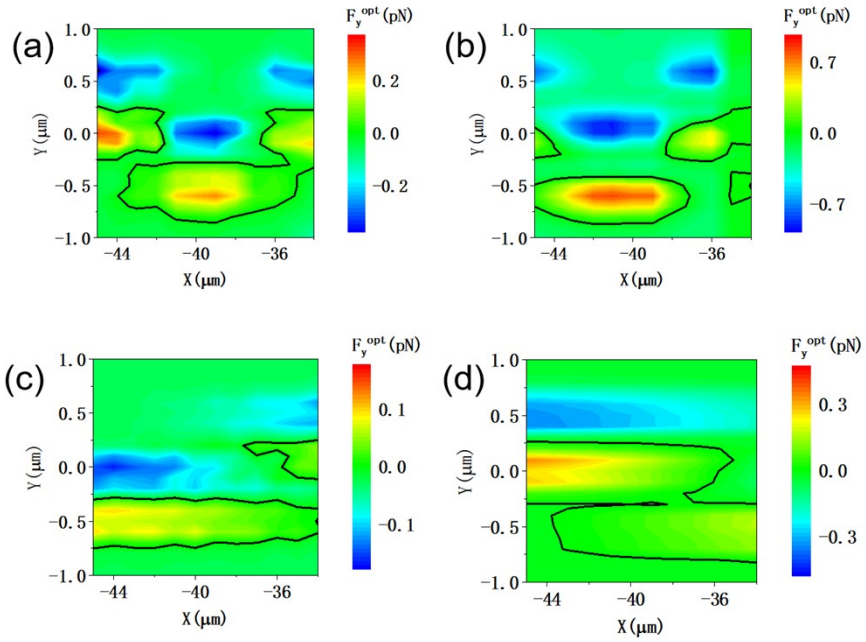

Fig S3. The analysis of optical gradient force (F_y^{opt}) on the (a) spherical particle (d_{sphere} = 0.5 μm) and (b) rod-shaped particle (d = 0.5 μm, l= 1.5 μm) for the amorphous state,

as well as (c) spherical (d_{sphere} = 0.5 μm) and (d) rod-shaped particles (d = 0.5 μm, l = 1.5 μm) for the crystalline state, where the particles are positioned 10 nm above the ONSWA.

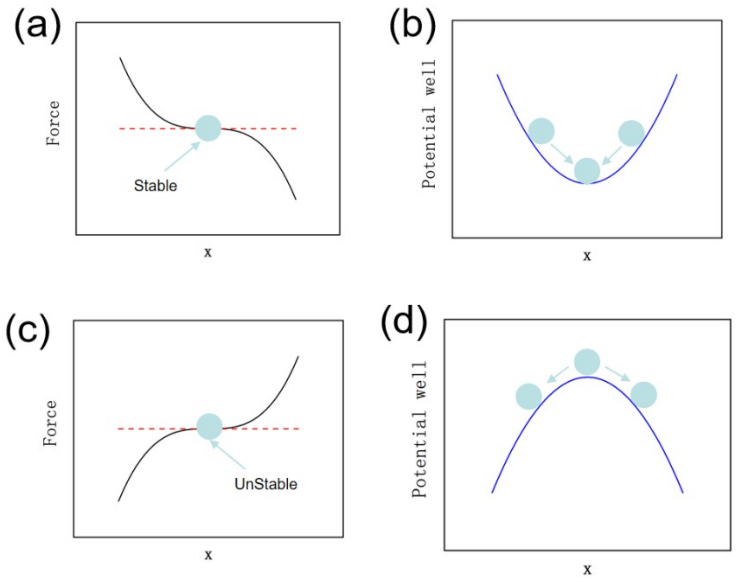

Fig. S4. Illustration of stable and unstable trapping locations. (a) The restoring forces occur on both sides of the stable trapping positions. (b) The potential well possesses a valley-like profile around the stable trapping position. (c) The deviating forces happen on one or both sides of the unstable trapping positions. (d)The potential well exhibits a peak around the stable trapping position thus releasing the particles.

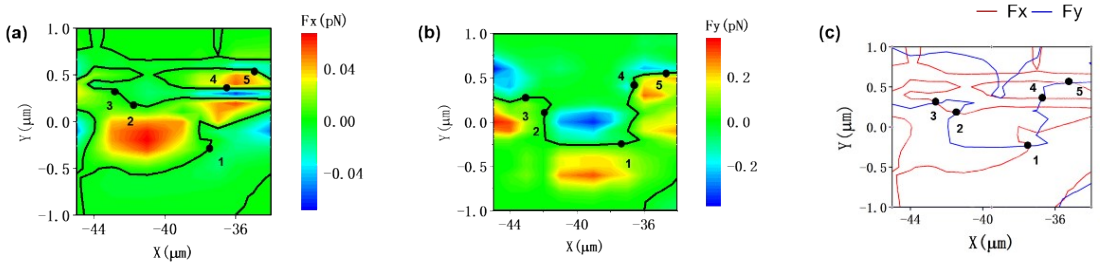

Fig. S5. Analysis of force and capturing locations of multiple spherical particles. (a, b) Maps of (a) F_x and (b) F_y with one spherical particle precaptured in location 1. (c) Intersections of contours of real capturing locations along the x- (red) and y-axes (blue) with one spherical particle precaptured in location 1. The precaptured spherical particle induces more capturing locations 2−5

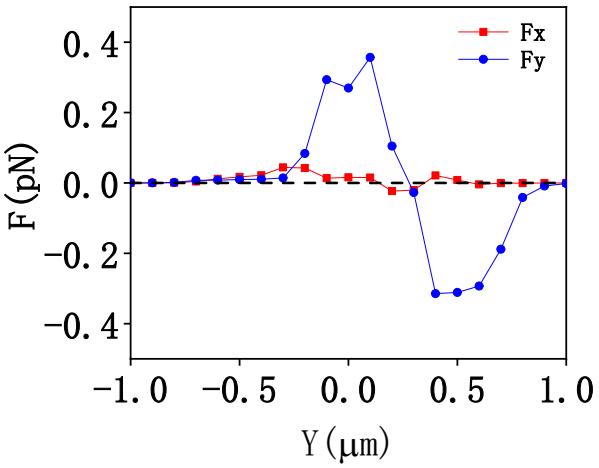

Fig S6. The simulated F_x and F_y on the rod-shaped particle at x = 0 while alternating the location along the y-axis.

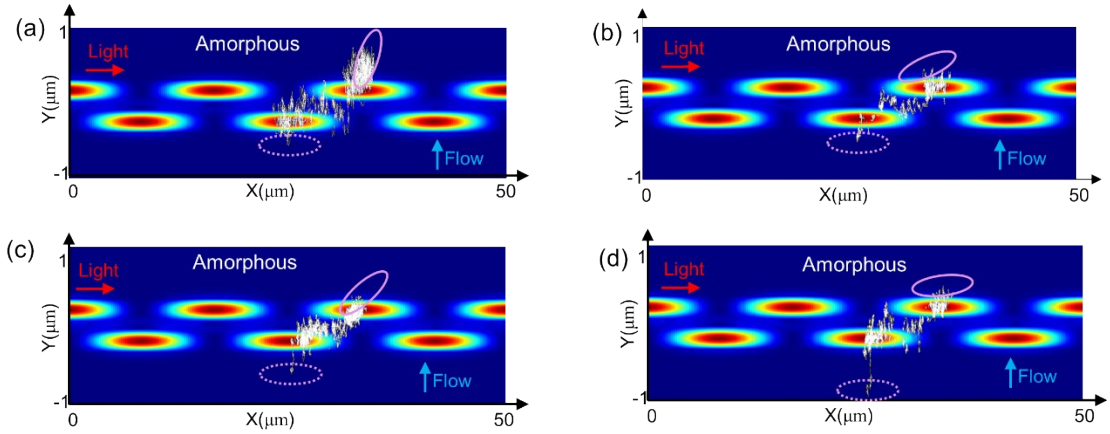

Fig. S7. Observation of the 100 ms trajectories of the polystyrene rod-shaped particles positioned 10 nm above the paired amorphous- Sb_2Se_3 waveguides at x = 25 μm while alternating the location along the *y*-axis for (a) y = -0.2 μm, (b) y = -0.4 μm, (c) y= -0.6 μm, and (d) y = -0.8 μm. The pink solid circles indicate the ends of the trajectories. The pink dotted line indicates the initial location of the particle.

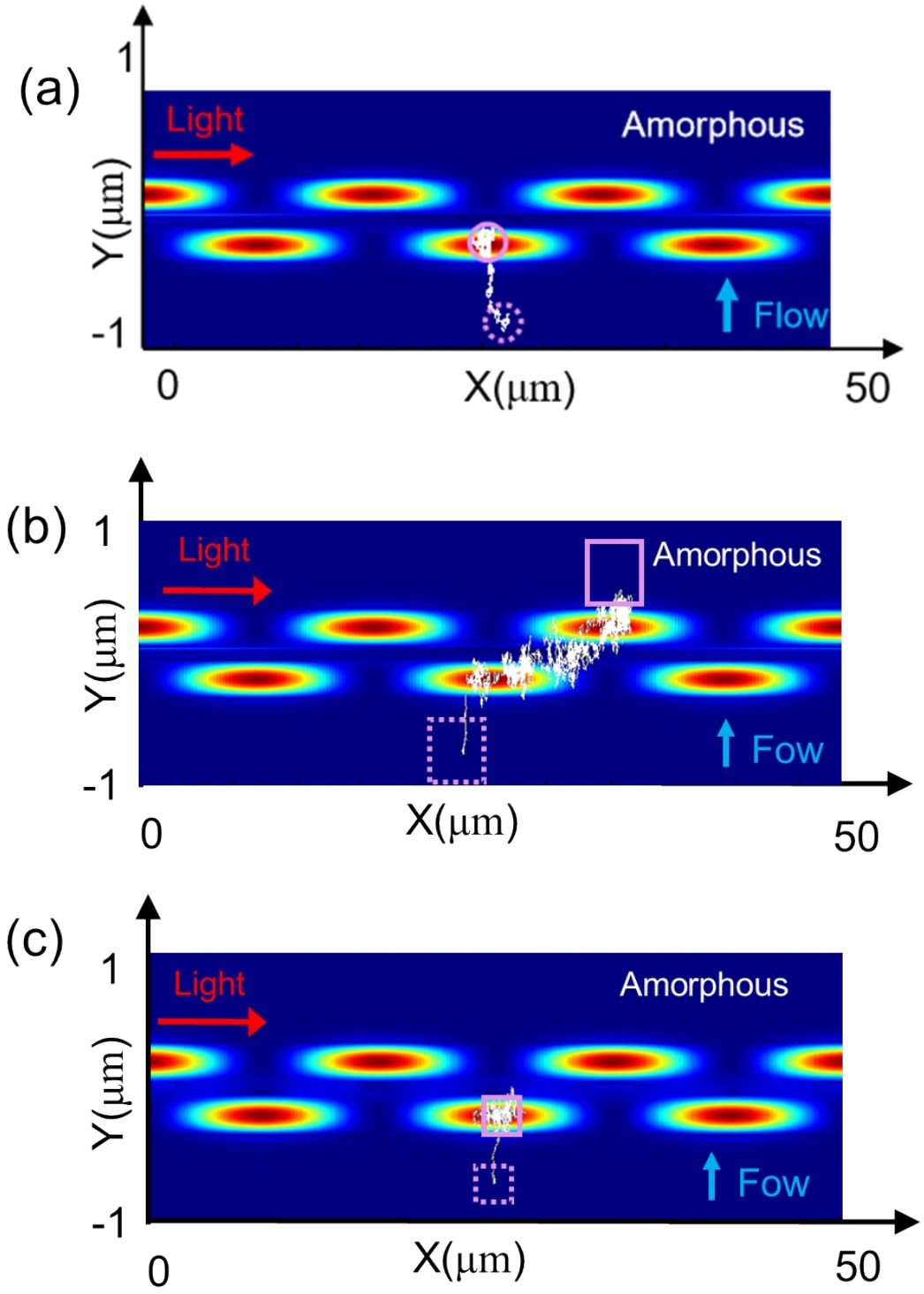

Fig. S8. Observation of the stability of polystyrene beads. The white lines show the 100 ms trajectories of the polystyrene (a) spherical (diameter of 0.5 μm), (b) cubic (side length = 1 μm), and (c) cubic (side length = 0.5 μm) shaped particles positioned 10 nm above the paired amorphous- Sb_2Se_3 waveguides. The pink solid circles indicate the ends of the trajectories. The pink dotted line indicates the initial location of the particle.

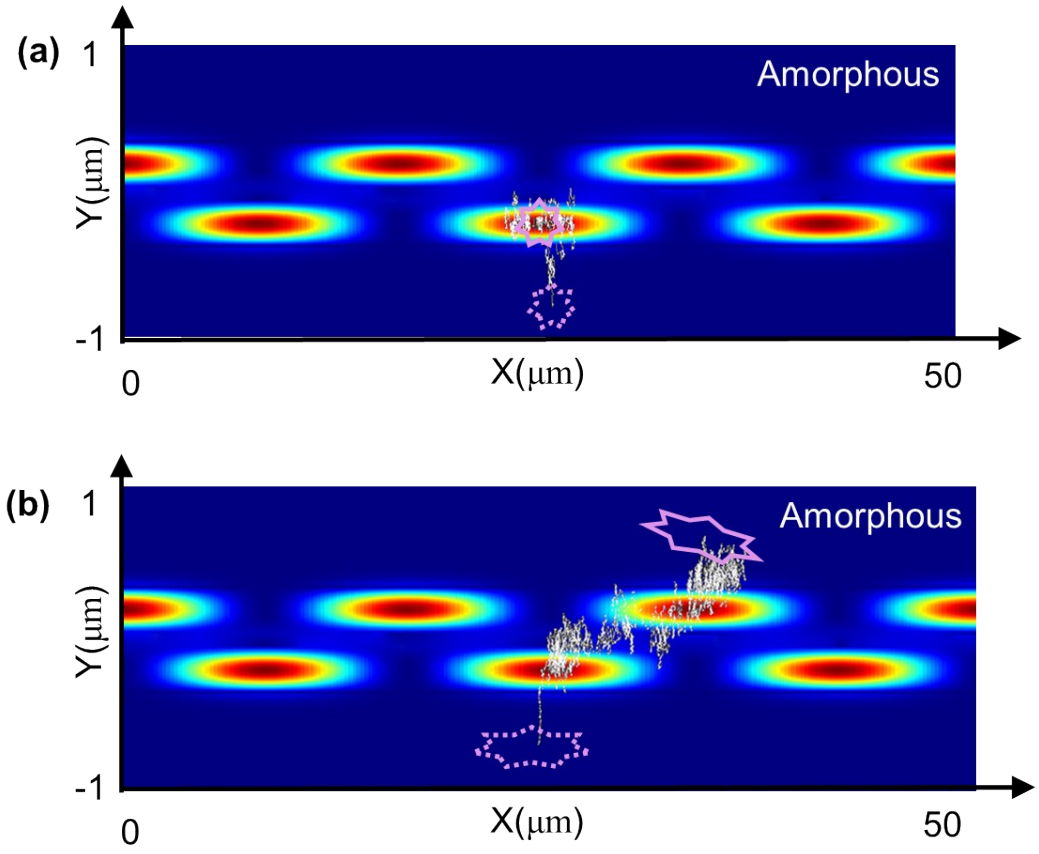

Fig. S9. Observation of the stability of polystyrene beads. The white lines show the 100 ms trajectories of the polystyrene imperfect (a) spherical and (b) rod-shaped particles positioned 10 nm above the paired amorphous- Sb_2Se_3 waveguides. The pink solid circles indicate the ends of the trajectories. The pink dotted line indicates the initial location of the particle.

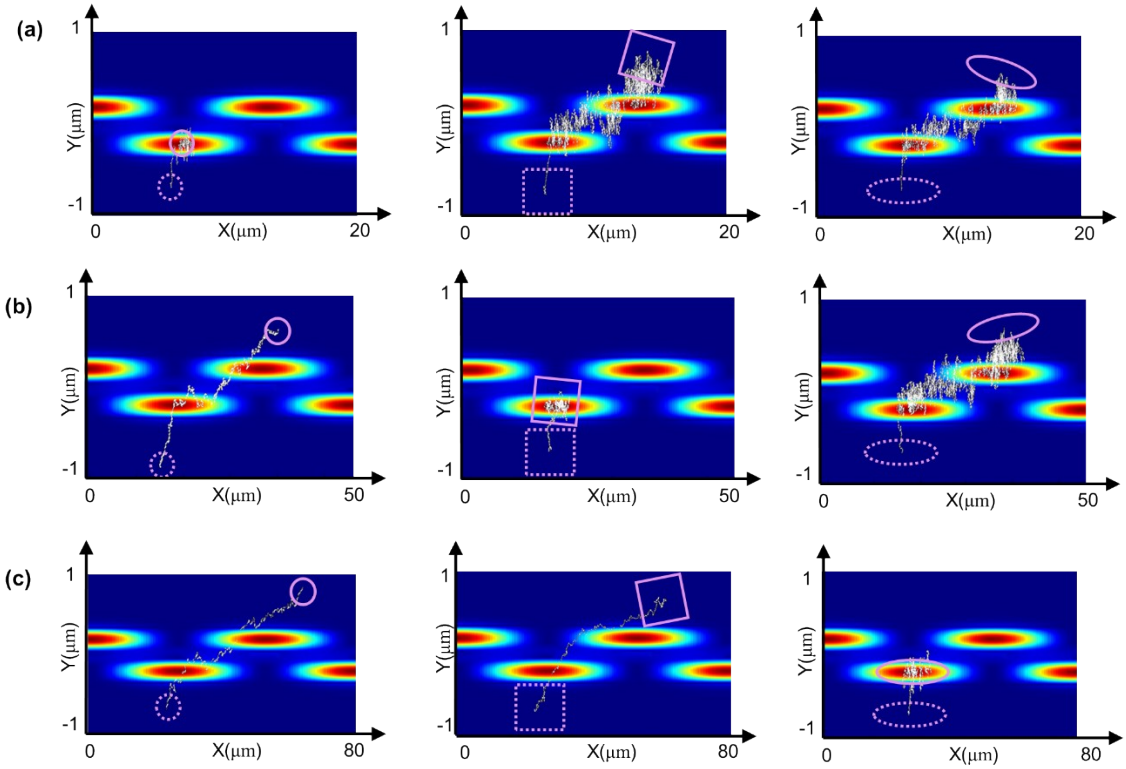

Fig. S10. Observation of the stability of left column: polystyrene spherical (d_{sphere} = 0.5 μm), central column: polystyrene cubic (d_{cubic} = 1 μm) , and right column: polystyrene rod-shaped particles (d = 0.5 μm, l = 1.5 μm) under the light fields. The white lines show the 100 ms trajectories of the polystyrene particles positioned 10 nm above the paired Sb_2Se_3 waveguides with (a) amorphous (g =0), (b) partial crystalline (g = 0.65), and (c) crystalline (g =1) states, respectively. The values of C_L were 7, 16, and 25 μm corresponding to g = 0, 0.65 , and 1, respectively.